Comparing and Contrasting the Effects of *Drosophila* Condensin II Subunit dCAP-D3 Overexpression and Depletion *in Vivo*

Emily Deutschman,*,† Jacqueline R. Ward,* Kimberly T. Ho-A-Lim,‡ Tyler J. Alban,§,‡ Dongmei Zhang, Belinda Willard,** Madeleine E. Lemieux,†† Justin D. Lathia,§,‡ and Michelle S. Longworth*,‡**

*Department of Inflammation and Immunity, Lerner Research Institute of Cleveland Clinic Cleveland, OH, 44195, †Department of Genetics and Genome Sciences, Case Western Reserve University Cleveland, OH, 44106, ‡Department of Molecular Medicine, Cleveland Clinic Lerner College of Medicine of Case Western Reserve University, Cleveland, OH 44195, §Department of Cellular and Molecular Medicine, and **Proteomics Core, Lerner Research Institute of Cleveland Clinic, Cleveland, OH 44195, and ††Bioinfo, Plantagenet, ON K0B 1L0, Canada

ORCID ID: 0000-0002-1313-1777 (M.S.L.)

ABSTRACT The Condensin II complex plays important, conserved roles in genome organization throughout the cell cycle and in the regulation of gene expression. Previous studies have linked decreased Condensin II subunit expression with a variety of diseases. Here, we show that elevated levels of Condensin II subunits are detected in somatic cancers. To evaluate potential biological effects of elevated Condensin II levels, we overexpressed the Condensin II subunit, dCAP-D3 in *Drosophila melanogaster* larval tissues and examined the effects on the mitotic- and interphase-specific functions of Condensin II. Interestingly, while ubiquitous overexpression resulted in pupal lethality, tissue specific overexpression of dCAP-D3 caused formation of nucleoplasmic protein aggregates which slowed mitotic prophase progression, mimicking results observed when dCAP-D3 levels are depleted. Surprisingly, dCAP-D3 aggregate formation resulted in faster transitions from metaphase to anaphase. Overexpressed dCAP-D3 protein failed to precipitate other Condensin II subunits in nondividing tissues, but did cause changes to gene expression which occurred in a manner opposite of what was observed when dCAP-D3 levels were depleted in both dividing and nondividing tissues. Our findings show that altering dCAP-D3 levels in either direction has detrimental effects on mitotic timing, the regulation of gene expression, and organism development. Taken together, these data suggest that the different roles for Condensin II throughout the cell cycle may be independent of each other and/or that dCAP-D3 may possess functions that are separate from those involving its association with the Condensin II complex. If conserved, these findings could have implications for tumors harboring elevated CAP-D3 levels.

KEYWORDS Condensin II; gene expression; mitosis; CAP-D3; development

THE three-dimensional organization of the genome is important for both efficient cellular division as well as for the regulation of gene transcription. In mitosis, proper packaging of DNA is essential for the symmetric segregation of genetic material. In interphase, the positioning of loci within the cell's nucleus can largely affect both the spatial and temporal expression of genes (Holwerda and de Laat 2012; Van Bortle and Corces 2012; Smallwood and Ren 2013; Dowen and Young 2014; Gorkin *et al.* 2014; Dekker and Mirny 2016). DNA is organized in a hierarchical manner, with chromosomes occupying their own discrete territories (Croft *et al.* 1999; Bolzer *et al.* 2005; Cremer and Cremer 2010). It has also recently been determined that individual chromosomes are organized into topologically associated domains (TADs), which contain genomic regions of higher intrachromosomal interaction frequency (Nora *et al.* 2013). Disruption of TADs and TAD boundaries can negatively affect gene expression, leading to both acquired diseases as well as developmental defects (Lupiáñez *et al.* 2015, 2016). In addition to intrachromosomal interactions, interactions between chromosomes

doi: https://doi.org/10.1534/genetics.118.301344
Manuscript received July 9, 2018; accepted for publication July 31, 2018; published Early Online August 1, 2018.
Available freely online through the author-supported open access option.
Supplemental material available at Figshare: https://doi.org/10.25386/genetics.6884690.
[1]Cleveland Clinic Lerner Research Institute 9500 Euclid Ave, NC2-133 Cleveland, OH 44195 216-444-8082. E-mail: longwom@ccf.org

through chromosome pairing or through contacts between interchromosomal loops can also influence gene expression (Apte and Meller 2012; Holwerda and de Laat 2012).

Condensin II is a multisubunit complex found in multicellular organisms that is necessary in both the establishment and maintenance of genome architecture throughout the cell cycle. In *Drosophila*, the Condensin II complex comprises two structural maintenance of chromosome (SMC) subunits, dSMC2 and dSMC4, and two chromosome-associated protein (CAP) subunits, the kleisin dCAP-H2 and the HEAT-repeat protein dCAP-D3 (Nasmyth and Haering 2005). Unlike mammalian Condensin II, the *Drosophila* CAP-G subunit has been shown to exclusively associate with the Condensin I complex (Herzog *et al.* 2013). Condensin II is most known for the role it plays in condensing DNA during mitosis (Steffensen *et al.* 2001; Ono *et al.* 2003, 2004; Hirota *et al.* 2004; Nasmyth and Haering 2005). Recent work has shown that Condensin II possesses important functions in interphase as well. In the fly, roles for Condensin II in chromosome territory formation and maintenance, TAD organization, and the repression of homologous chromosome pairing have been identified (Hartl *et al.* 2008; Bauer *et al.* 2012; Joyce *et al.* 2012; Li *et al.* 2015). Work from our laboratory in both *Drosophila* and human cells has shown that depletion of the CAP-D3 subunit of Condensin II also results in the deregulation of gene expression (Longworth *et al.* 2012; Schuster *et al.* 2013, 2015; Klebanow *et al.* 2016). Studies from other laboratories have also implicated CAP-H2 and CAP-G2 in gene regulation (Xu *et al.* 2006; Hartl *et al.* 2008; Rawlings *et al.* 2011). Chromatin-immunoprecipitation (ChIP) and ChIP-sequencing (ChIP-seq) experiments have identified Condensin II binding sites at regions flanking target gene loci (Rawlings *et al.* 2011; Longworth *et al.* 2012; Pan *et al.* 2013; Schuster *et al.* 2013, 2015; Klebanow *et al.* 2016), at enhancer elements (Dowen *et al.* 2013), and at TAD boundaries (Li *et al.* 2015; Yuen *et al.* 2017). Additionally, loss of Condensin II has been shown to affect the chromatin landscape proximal to the genes it regulates (Rawlings *et al.* 2011; Schuster *et al.* 2013), but the direct mechanisms by which Condensin II regulates gene expression and the extent to which the condensation function of Condensin II affects the gene regulatory functions are still not well understood.

Both genomic instability and the aberrant regulation of gene expression have been linked to cancer. Since Condensin II is a key regulator of genome architecture, plays a role in the regulation of gene expression, and has been implicated in tumor development in both mice (Woodward *et al.* 2016) and humans (Ham *et al.* 2007; Leiserson *et al.* 2015), we examined CAP-D3 expression patterns in human somatic cancers using the COSMIC database (http://cancer.sanger.ac.uk/cosmic). In finding that elevated CAP-D3 levels were present in many different somatic tumors, we sought to characterize the effects of higher dCAP-D3 expression levels *in vivo*. Here we show that overexpression of dCAP-D3 in *Drosophila* results in the formation of protein aggregates in both dividing and nondividing tissues. Our data also indicate that, similar to underexpression, overexpression of dCAP-D3 accompanied by aggregate formation slows mitotic progression *in vivo* as a result of lags identified in prophase. Interestingly, we also show that overexpression of dCAP-D3 results in changes to gene expression in a pattern opposite to what is observed in dCAP-D3-deficient tissues. Our findings juxtapose the effects of dCAP-D3 overexpression and depletion in dividing and nondividing tissues. If conserved, these results could shed light on possible mechanisms by which elevated CAP-D3 levels potentially contribute to both developmental defects and tumor development.

Materials and Methods

Fly strains

All stocks were maintained at 25° on standard dextrose medium. For RNA-sequencing (RNA-seq) experiments, the w^{1118} (Bloomington Stock Center 5905) stock served as a wild-type control. *dCap-D3* mutant larvae for this experiment were homozygous for the hypomorphic *c07081* allele which was generated in the w^{1118} line (Thibault *et al.* 2004) (w; $dCap\text{-}D3^{c07081/c07081}$; Harvard Exelixis c07081). Quantitative real-time PCR (qRT-PCR) validation of RNA-seq-identified targets were also performed in these lines as well as in a line transheterozygous for the *c07081* allele and *Δ25* chromosomal deletion. Progeny were generated by crossing heterozygous $dCap\text{-}D3^{c07081}/Cyo\text{-}GFP$ virgins with *Δ25/Cyo-GFP* males (Bloomington Stock Center 25). For live imaging experiments, *w*;P{His2Av-mRFP1}III.1* (Bloomington Stock Center 23650) larvae were used as wild-type controls. The *His2Av-mRFP* allele was crossed into $dCap\text{-}D3^{c07081}/Cyo\text{-}GFP$ flies to generate a stock with the genotype of $dCap\text{-}D3^{c07081/c07081}$;*P{His2Av-mRFP1}III.1* used for imaging analysis. Imaging was also performed in transheterozygous tissue generated by crossing $dCap\text{-}D3^{c07081}/cyo\text{-}GFP$ females with *Δ25/cyo-GFP* males. Ubiquitous overexpression and overexpression in the salivary glands and wing discs was accomplished by crossing β-*tubulin-GAL4*, *SGS-GAL4*, or *Nubbin-GAL4* males with *pUASt-GFP-dCAP-D3*, *pUASt-FLAG-HA-dCAP-D3*, pUASg-dCAP-D3, *pUASt-GFP*, or *pUASt-FLAG-HA* virgins. GFP-dCAP-D3, FLAG-HA-dCAP-D3, FLAG-HA, and GFP overexpression stocks were generated using the gateway system as previously described in Longworth *et al.* (2012). pUASg-dCAP-D3 were acquired from FlyORF (M{UAS-Cap-D3.ORF} ZH-86Fb, F001285). For live imaging in the wing disc, *Nubbin-GAL4* flies were crossed with *w*;P{His2Av-mRFP1}-III.1* flies to generate a *Nubbin-GAL4;P{His2Av-mRFP}III.1* stock. Males from this stock were then crossed with *pUAst-GFP-dCAP-D3* or *pUASt-GFP* (control) virgins to drive expression in the wing disc pouch.

Immunofluorescence

All tissues were fixed in 4% paraformaldehyde/0.5% Triton X-100 for 25 min with rocking at room temperature. Stained tissues were washed with 0.1% PBS-Triton, blocked in 0.1% PBS-Triton/1%BSA, and incubated with primary antibody in

block buffer [dCAP-D3, 1:50 (Longworth *et al.* 2008); lamin, 1:100 (Developmental Studies Hybridoma Bank ADL67-10); HA, 1:500 (Biolegend); CID, 1:500 (Blower and Karpen 2001); PH3, 1:500 (06570 Millipore, Bedford, MA, or abcam14955] overnight at 4°. The following day, samples were washed and incubated with secondary antibody (1:500, Alexa Fluor; Thermo Fisher, San Jose, CA). Tissues were mounted in Vectashield with DAPI prior to imaging.

Live imaging

Protocols were adapted from what was previously described in Handke *et al.* (2014) and Poulton *et al.* (2014). Briefly, wing discs were dissected from third instar larvae at room temperature and placed apical side up onto an oxygen-permeable Lumox dish 50 (Sarstedt) in a base media [Schneider's media (GIBCO, Grand Island, NY), 5% fly extract (*Drosophila* Genomics Resource Center), 6.2 μg/ml bovine insulin, and 1% penicillin/streptomycin] supplemented with 200 μg/ml bovine insulin. Spacers of 1 μm in thickness were placed adjacent to the disc and a poly-L-lysine-coated coverslip was placed on top. Coverslips were sealed with Halocarbon oil 700 (Sigma Chemical, St. Louis, MO) around the edges. Discs were allowed to settle for 30 min, after which they were imaged with a 40× water objective for up to 3 hr.

Imaging

Unless otherwise noted, all imaging was performed using a Leica SP5 confocal/multi-photon microscope that was purchased with partial funding from National Institutes of Health Scientific Interest Groups grant 1S10RR026820-01.

Immunoprecipitation and mass spectrometry

Antibodies (4 μg GFP, 1 μl IgG preserum) were incubated with Protein A Dynabeads for 4 hr at room temperature with rocking. Six-hundred pairs of salivary glands per genotype were homogenized in either a low salt (150 mM NaCl, 50 mM Tris, pH 7.5, 1 mM EDTA, 0.1% Triton, 10% glycerol, 1 mM DTT, 1× protease inhibitor cocktail) or high salt (300 mM NaCl, 50 mM Tris, pH 7.5, 1 mM EDTA, 0.1% Triton, 10% glycerol, 1 mM DTT, 1× protease inhibitor cocktail) lysis buffer. Samples were adjusted to 650μL, and 200μL of lysate was used per IP, which was performed overnight at 4° with rocking. After washes, samples were boiled off of beads in 30 μl Laemmli buffer for 5 min. Equal volumes of sample were run on an SDS-polyacrylamide gel and stained with Gel CodeBlue (Thermo Fisher) overnight. Protein bands from control and IP samples were excised from the gel, reduced with DTT, and alkylated with iodoacetamide prior to the in-gel digestion. All bands were digested using trypsin by adding 5 μl of 10 ng/μl trypsin in 50 mM ammonium bicarbonate and incubating overnight at room temperature. The peptides that were formed were extracted from the gel pieces. These extracts were evaporated in a SpeedVac and then resuspended in 1% acetic acid for liquid chromatography–mass spectrometry (LC-MS) analysis. The LC-MS system was a Finnigan LTQ-Obitrap Elite hybrid mass spectrometer system (Thermo Fisher). The HPLC column was a Dionex 15 cm × 75 μm inner diameter Acclaim Pepmap C18, 2 μm capillary chromatography column. A 5-μl aliquot of the extract was injected and the peptides eluted from the column by an acetonitrile/0.1% formic acid gradient at a flow rate of 0.3 μl/min. The digest was analyzed using the data-dependent multitask capability of the instrument, acquiring full-scan mass spectra to determine peptide molecular weights and product-ion spectra to determine amino acid sequence in successive instrument scans. The data were analyzed by using centromere identifier (CID) spectra collected in the experiment to search the *Drosophila* reference sequence database (27,588 entries), using the programs Mascot (Matrix Science, London, United Kingdom) and Sequest (Thermo Fisher), and more specifically against the sequence of dCAP-D3 using the program Sequest. Protein and peptide identification was validated using the program Scaffold (Proteome Software, Portland, OR). Protein identifications were accepted if they could be established at >99.9% probability using the Protein Prophet algorithm and contained at least two identified peptides. The proteins identified in the control and IP samples were compared using the total number of spectra (spectral counts) identified in the LC-MS/mass-spectrometry analysis and putative dCAP-D3 binding partners are proteins preferentially identified in the IP sample compared to control. The Orbitrap Elite Instrument was purchased via a National Institutes of Health shared instrument grant, 1S10RR031537-01.

Polytene squashes

Salivary glands were dissected from larvae in fresh formaldehyde fixation buffer (0.15 M PIPES, 3 mM $MgSO_4$, 1.5 mM EGTA, 1.5% NP-40, 2% formaldehyde). Dissection and fixation were both performed in 2–3 min. Glands were incubated in 0.2% Triton-PBS (PBT) for 2–3 min and then transferred to 50% glycerol for an additional 5 min. After transferring to a fresh drop of 50% glycerol on a coverslip, a poly-L-lysine-coated slide was placed over the top of the glands and squashing and spreading was carried out by pressing on the cover glass with a pencil. Slides were flash frozen in liquid nitrogen and the coverslip removed with a razor blade. Slides were rehydrated in PBT and blocked in PBT plus 0.2% BSA and 0.5% goat serum prior to the addition of primary antibody as described above. Slides were stained with DAPI (1:100) prior to imaging.

RNA isolation

RNA was isolated from *Drosophila* larval tissue using standard TriZol methods. Each salivary gland and wing disc sample consisted of 50 and 150 tissues, respectively. Samples were cleaned and concentrated using the QIAGEN (Valencia, CA) Mini RNeasy Kit.

RNA-seq

RNA was isolated as described above. Directional (wing disc) or nondirectional (salivary gland) complementary-DNA (cDNA) libraries (50 bp, paired end) were made at the University of Chicago Genomics Core and sequenced on an Illumina

HiSeq2500, according to standard protocols. Raw data files (48–158 million paired reads per sample) are available under the National Center for Biotechnology Information (NCBI) Gene Expression Omnibus accession number GSE116419. Adapters and low quality bases were trimmed with Trim Galore version 0.3.3 (https://www.bioinformatics.babraham.ac.uk/projects/trim_galore/) and controlled for quality with FastQC version 0.11.3 (https://www.bioinformatics.babraham.ac.uk/projects/fastqc/) before alignment to the *Drosophila* genome assembly BDGP6 [Flybase FB2015_01 released February 24, 2015, with Ensembl 6.04 annotations (dos Santos *et al.* 2015)] using BWA aln/sample (version 07.12) (Li and Durbin 2009) with default settings. Unmapped reads were aligned using TopHat version 2.0.8b (Kim *et al.* 2013) (-r 150 –mate-std-dev 100 –b2-sensitive –I 5000) to retrieve splice junctions. HTSeq version 0.6.1 (Anders *et al.* 2015) was used to count transcripts. Picard tools (version 1.119; http://broadinstitute.github.io/picard) were used to convert formats and to merge alignment files. Prior to differential expression (DE) analysis, gene-level counts were filtered such that at least one sample had >0.5 read per million mapped (11,021/16034, 68.7% retained). Thereafter, tissue expression differences were assessed separately comparing *dCap-D3* mutants to wild type in each case. After a first-pass DE analysis with edgeR version 3.16.5 (McCarthy *et al.* 2012), a control set consisting of genes with false discovery rate (FDR) >0.1 and absolute $\log_2$ fold change (logFC) <1.1 was used with RUVg (estimating the factors of unwanted variation using control genes) ($k = 1$) to identify unwanted variation [RUVSeq version 1.8.0 (Risso *et al.* 2014)]. The second-pass edgeR analysis included the RUVg correction factor in the model matrix. Genes with FDR <0.05 and absolute logFC >1 were retained for further analysis. DAVID version 6.8 (Huang *et al.* 2009) was used for gene ontology (GO) enrichment analysis of the DE gene lists using all *Drosophila melanogaster* genes as background.

qRT-PCR

cDNA was made with 1 μg of RNA per 50 μl reaction using the TaqMan Reverse Transcription Kit (Life Technologies). qRT-PCR was performed as described in Longworth *et al.* (2012) using a Roche LightCycler480. Primer sequences are as follows: *CG32073*-F: GCCATTTGCCTGTATTCCGTT, *CG32073*-R: GTAGTCGAGGTGCCAGTGCC AGTT; *CG32071*-F: CTGGTTG TCCTGTCCTCGCA, *CG32071*-R: CAGCCGTAGTGGTAGT GG TG; *CG13560*-F: AAGTACGGCCACTGGCAGCA, *CG13560*-R: CGAAGAGCTACTGCT GGAGC; *CG17147*-F: CTGGCCTACG GGACACATCC, *CG17147*-R: CCAGCAAGGGTAGT TGCGTG; *CecC*-F: CAATCGGAAGCCGGTTGGCTG, *CecC*-R: GCGCAAT TCCCAGTCCTT GAATGG; *HP1D3csd*-F: GGGAGTTCACAA TTCGGCTCGG, *HP1D3csd*-R: GCGGCACGT; *Rp49*-F: TACAGG CCCAAGATCGTGAAG, *Rp49*-R: GACGCAC TCTGTTGT CGATACC.

Data availability

Supplemental Material, File S1 contains supplemental methods and supplemental file legends. Figures S1–S10 are supplemental figures. Table S1 is a list of DE genes identified by RNA-seq. Table S2 is a list of commonly deregulated target genes. Files S2–S7 are movies captured from live imaging experiments. Gene expression data are available under the NCBI Gene Expression Omnibus accession number GSE116419. Supplemental material available at Figshare: https://doi.org/10.25386/genetics.6884690.

Results

CAP-D3 expression levels are elevated in human somatic cancers

Condensin II plays an important role in organizing the genome throughout the cell cycle. As loss of CAP-D3 is associated with chromosome missegregation (Hartl *et al.* 2008; Longworth *et al.* 2008), we examined CAP-D3 levels in a panel of 9144 somatic cancers (COSMIC database) and were surprised to find that a greater percentage of tumors exhibited elevated rather than reduced levels of CAP-D3, based on Z-scores calculated from a population norm (Figure 1A) (Forbes *et al.* 2017). In fact, elevated levels of CAP-D3 were observed in 507 of the 9144 year (5.5%) somatic cancers tested, whereas only 91 of the 9144 tumors (1%) exhibited decreased levels of CAP-D3. Of the 507 tumors with increased CAP-D3 expression, the highest number were found in the lung (19%), breast (11%), and central nervous system (9%) (Figure 1B). Increased levels of other Condensin II subunits were also observed in tumors (Figure 1A), whereas lower levels of the tumor suppressor protein p53 was observed more often in somatic tumors (Figure 1A).

Overexpression of dCAP-D3, in vivo, results in the formation of nucleoplasmic aggregates

It is possible that elevated levels of Condensin II subunits are more frequently observed in tumors because higher Condensin II levels are required to accommodate the increase in cellular division that occurs in tumors. Interestingly, through The Cancer Genome Atlas (TCGA) analysis, we observed that individuals possessing low-grade gliomas (a type of central nervous system tumor with a low mitotic index) expressing higher levels of Condensin II subunits, on average, exhibited lower survival rates compared to individuals with low-grade gliomas expressing lower levels of Condensin II subunits (Figure S1, A–C). In contrast, TCGA analysis of survival rates for patients possessing glioblastomas (a type of high-grade glioma with a high mitotic index) expressing higher levels of Condensin II subunits did not reveal any significant differences when compared to patients possessing glioblastomas expressing lower levels of Condensin II subunits (Figure S1, D–F). These analyses demonstrate that elevated levels of Condensin II subunits are observed in tumors with lower numbers of mitotic events and may negatively affect patient survival.

It is also possible that elevated Condensin II levels might actually result in phenotypes that could lead to tumor development and/or progression. To investigate this second

A

PROTEIN EXPRESSION IN SOMATIC CANCERS				
Gene	Number of Cancers Overexpressing	Percent Overexpressing	Number of Cancers Underexpressing	Percent Underexpressing
CAP-D3	507	5.5	91	1.0
CAP-H2	492	5.4	115	1.3
CAP-G2	781	8.5	27	0.30
SMC2	499	5.5	16	0.17
SMC4	1088	11.9	17	0.19
p53	402	4.4	528	5.8

B

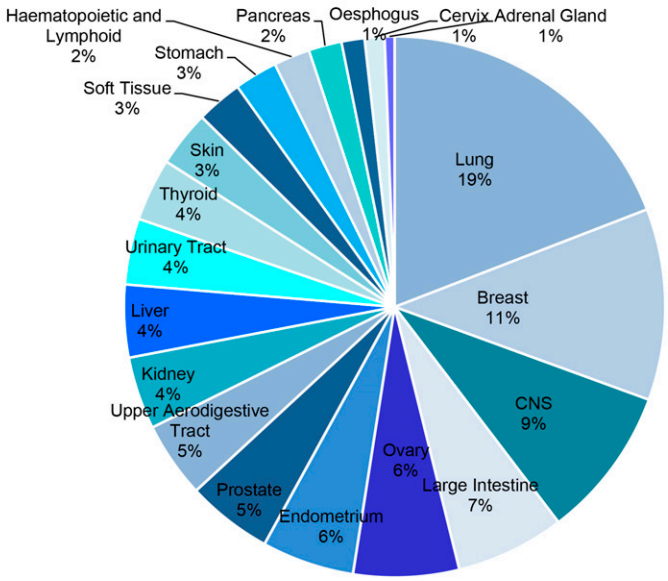

Figure 1 CAP-D3 levels are altered in somatic cancers. (A) Percentage of somatic cancers that exhibit elevated and lower levels of Condensin II proteins using the COSMIC database (http://cancer.sanger.ac.uk/cosmic). (B) Pie chart of different types of cancers that exhibit elevated CAP-D3 levels. Data were obtained using the COSMIC database.

possibility, we sought to assess the consequences of higher CAP-D3 levels on cellular division and in transcriptional regulation *in vivo* in *D. melanogaster*. Toward this end, we overexpressed dCAP-D3 using a GFP-tagged *Cap-D3* allele, which we have previously published to be able to rescue a loss-of-function dCAP-D3 phenotype caused by the loss of dCAP-D3-mediated ability to repress enhancer activity and gene transcription (Klebanow *et al.* 2016). dCAP-D3 overexpression was confirmed by Western blotting using the ubiquitous β-tubulin-GAL4 driver to promote expression of a GFP-dCAP-D3 or GFP control transgene (Figure S2). Using the SGS-GAL4 and Nubbin-GAL4 drivers, we expressed either GFP-dCAP-D3 or GFP in the salivary glands and in the wing disc pouch to characterize the effects of dCAP-D3 overexpression in a nondividing and dividing tissue type, respectively. Immunofluorescence experiments showed that overexpression of dCAP-D3 in both tissues resulted in the formation of GFP-dCAP-D3 aggregates that were not present when only GFP was expressed (Figure 2, A and B). The aggregates were found solely in the nucleus and appeared to predominantly inhabit the interchromatin space in cells from both tissues, however faint GFP-dCAP-D3 signal was observed colocalizing with DAPI. The formation of GFP-dCAP-D3 aggregates was most likely not an artifact of GFP-tag fusion to dCAP-D3 protein, as overexpression of FLAG-HA tagged and untagged dCAP-D3 also resulted in aggregate formation (Figure S3 and Figure S4). Upon examination of aggregate numbers, we observed a significant variation ranging between 1 and 10 GFP-dCAP-D3 aggregates present in each salivary gland nucleus (Figure S5). Interestingly, only one GFP-dCAP-D3 aggregate was ever observed in a given wing disc nucleus, with some cells exhibiting a complete absence of GFP-dCAP-D3 aggregates. To determine if this discrepancy in aggregate number between salivary glands and wing discs was a result of using GAL4 drivers of different strengths, we used β-tubulin-GAL4 to ubiquitously overexpress GFP-dCAP-D3 at higher levels in both tissues. In both tissues, the aggregates appeared to be more interconnected, suggesting that higher expression driven by the stronger β-tubulin-GAL4 driver may increase the size of and/or interactions between aggregates. Salivary gland nuclei from these larvae, however, still exhibited a higher number of distinct GFP-dCAP-D3 aggregates and each wing disc nucleus still contained one GFP-dCAP-D3 aggregate, with some nuclei exhibiting a complete absence of aggregates (Figure 6, A and B). Together, the observed difference in aggregate number combined with the complete absence of aggregates in some wing disc cells suggests that there may be a tissue- or cell-specific component acting to regulate the formation of these GFP-dCAP-D3 structures.

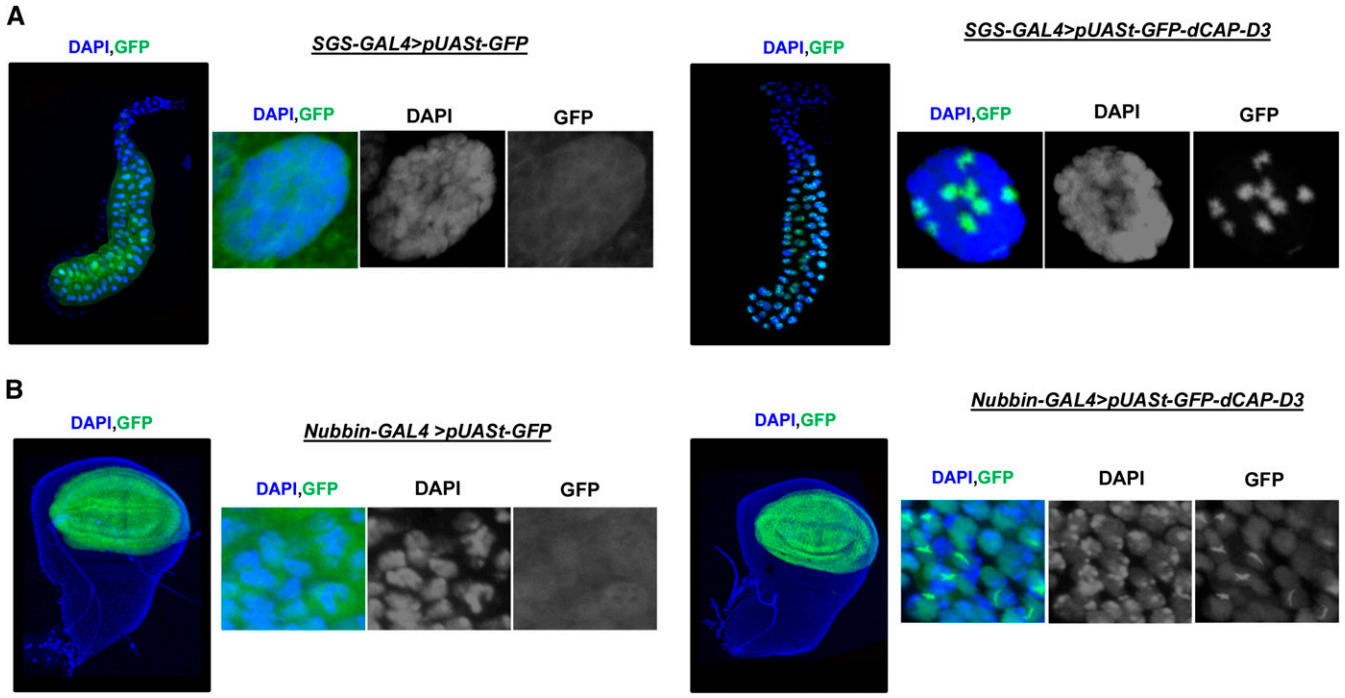

Figure 2 GFP-dCAP-D3 overexpression results in protein aggregate formation. Fluorescence analyses were performed in third instar larval (A) salivary glands and (B) wing discs expressing GFP (left panel, green) or GFP-dCAP-D3 (right panel, green). SGS-GAL4 was used to drive expression in salivary glands and Nubbin-GAL4 to drive expression in the wing disc. DAPI staining of nuclei is shown in blue. Magnified images are shown to the right of each larger image of the whole tissue.

Both underexpression and overexpression of dCAP-D3 significantly affect mitotic timing

Condensin II functions to ensure the uniform condensation of chromosomes prior to cellular division (Ono *et al.* 2003, 2004; Hirota *et al.* 2004; Longworth *et al.* 2008). This function is essential for facilitating equal chromosome segregation (Hartl *et al.* 2008; Longworth *et al.* 2008). Work in HeLa and DT-40 chicken cells has shown that depleting CAP-D3 can alter mitotic progression (Hirota *et al.* 2004; Abe *et al.* 2011; Bakhrebah *et al.* 2015). To determine whether this occurs *in vivo*, we performed live cell imaging in wing discs expressing an RFP-tagged histone variant (His2aV-mRFP) explanted from third instar larvae that expressed the previously characterized (Longworth *et al.* 2008, 2012) mutant *dCap-D3*$^{c07081/c07081}$ allele. From imaging analyses, we observed an increase in the average time that it took dCAP-D3-deficient cells to progress from the initial onset of observed condensation to the formation of the metaphase plate (Figure 3, A and B; File S2; and File S3). Similar to what has been shown in other organisms, decreasing dCAP-D3 expression also appeared to affect chromosome segregation, as a small but significant lag from metaphase-plate formation to the onset of anaphase was also observed (Figure 3, A and B). While omitted from the averaging, we witnessed extreme events in which chromosomes took up to 50 min to resolve when dCAP-D3 levels were depleted (File S4). Imaging analyses of wing discs explanted form *dCap-D3*$^{c07081/\Delta 25}$; *His2aVmRFP* larvae recapitulated the metaphase to anaphase lags observed in *dCap-D3*$^{c07081/c07081}$ discs, but not the prophase to metaphase lags (Figure S7 and File S5). This is surprising as we have previously reported that *dCap-D3*$^{c07081/\Delta 25}$ larval brains exhibit condensation defects (Longworth *et al.* 2008). As the *Δ25* allele is a second chromosome deletion that results in the loss of 63 other genes and regulatory RNAs in addition to *dCap-D3*, including the B-type lamin *lamDm0*, it is possible that decreased expression of these other factors could influence mitotic progression, thus skewing the prophase timing results. Indeed, the nuclear lamina has been shown to be important for regulating chromosome movement during meiotic prophase in *Caenorhabditis elegans* (Link *et al.* 2018), but whether it plays similar roles in mitotic cells is unknown.

Since we identified lags in mitosis in these developing discs, we asked whether *dCap-D3*$^{c07081/c07081}$ flies would also exhibit gross changes in development. To test this, we analyzed eclosion rates in both wild-type and *dCap-D3* mutant flies. We found that, on average, *dCap-D3* mutants took significantly longer to emerge from their pupal casing compared to their wild-type counterparts (Figure S8A), suggesting that lags in mitosis at the cellular level may be contributing to a more global developmental delay. Additionally, we also observed that adult *dCap-D3* mutant males and females (Figure S8B) exhibited a decrease in overall body weight compared to wild-type adults, which may imply that a decrease in the rate of mitosis could translate to a decrease in cell number.

Next, to determine the effects of increased levels of dCAP-D3 on mitotic progression, we used Nubbin-GAL4 to drive

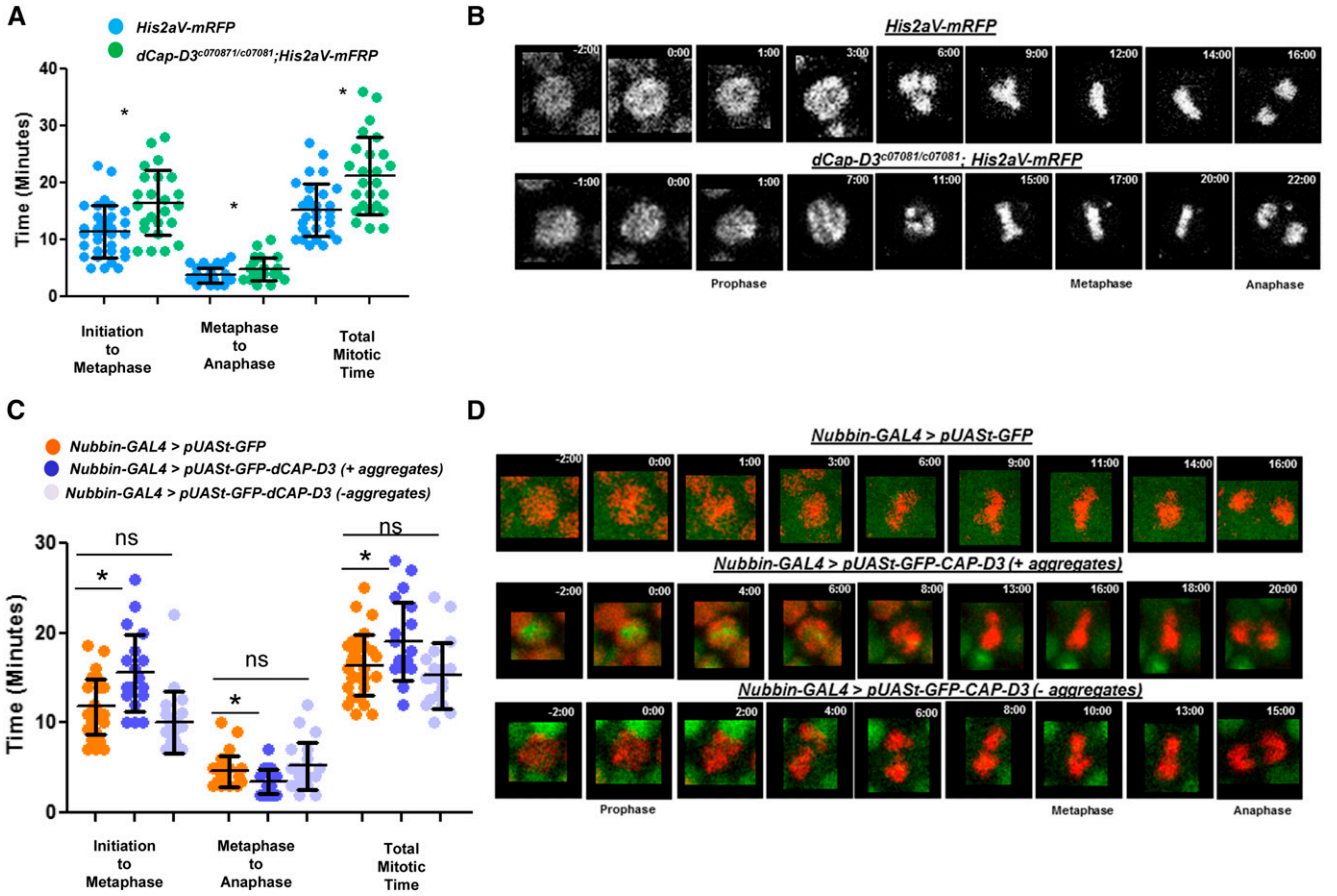

Figure 3 Altering levels of dCAP-D3 influences mitotic progression. (A) Plot showing mitotic progression times in control (*His2aV*-mRFP). Blue ●: three discs, *n* = 32 cells, and *dCap-D3* mutant (*dCap-D3*$^{c07081/c07081}$; *His2aV-mRFP*). Green ●: three discs, *n* = 25 cells wing discs. (B) Stills of a representative mitotic event in a control (top row) and in a *dCap-D3* mutant (bottom row) wing disc. (C) Plot showing mitotic progression times in discs expressing control GFP (*Nubbin-GAL4 > pUASt-GFP*). Orange ●: three discs, *n* = 30 cells, discs expressing GFP-dCAP-D3 protein where aggregates are observed (*Nubbin-GAL4 > pUASt-GFP-dCAP-D3*). Purple ●: four discs, *n* = 20, and discs expressing GFP-dCAP-D3 protein where aggregates are not observed. Lilac ●: three discs, *n* = 20 cells. (D) Stills of a representative mitotic event in a wing disc expressing GFP (top row), a wing disc expressing GFP-dCAP-D3 where aggregates are present (middle row), and a wing disc expressing GFP-dCAP-D3 where aggregates are not observed (bottom row). * $P < 0.05$.

expression of GFP-tagged dCAP-D3 in the wing disc pouch in third instar larvae of the *w*; *His2Av-mRFP* background. Using only cells harboring GFP-dCAP-D3 aggregates for analysis, we—unexpectedly—again observed a lag in the time it took from the onset of DNA condensation to metaphase plate formation when dCAP-D3 was overexpressed as compared to GFP expression alone (Figure 3, C and D; File S6; and File S7). This, however, was not the case for cells that overexpressed GFP-dCAP-D3 but lacked aggregates, as a significant change in mitotic timing was not observed in these cells (Figure 3, C and D). Notably, while dCAP-D3-deficient wing disc cells exhibited lags in both early and late mitosis (Figure 3A), cells that overexpressed dCAP-D3 actually exhibited a significant acceleration in timing from metaphase to sister chromatid resolution when aggregates were present, but no change in timing when they were absent. (Figure 3, C and D; File S6; and File S7). Interestingly, GFP-dCAP-D3 aggregates disappeared after the appearance of the metaphase plate, which may be due to degradation or dissipation into the cytoplasm as a result of partial nuclear envelope breakdown. Like dCAP-D3-deficient cells, however, delays in total mitotic time were again only observed in dCAP-D3-overexpressing wing disc cells that possessed aggregates (Figure 3, C and D). The fact that timing defects are observed only in cells where aggregates are present suggests that it is the aggregation of dCAP-D3 that drives the phenotype.

Chromosome condensation has previously been shown to begin at centromeres and progress toward telomeres as mitosis continues (Hendzel *et al.* 1997). To determine whether altering dCAP-D3 levels perturbs this order, we immunostained dCAP-D3-deficient and -overexpressing wing discs with antibodies against the phosphorylated serine 10 residue of histone 3 (PH3) to detect condensed chromatin and centromere protein A (CENP-A/CID) to label centromeres (Figure 4, A and B). Our results show that regardless of dCAP-D3 levels, wing disc cells exhibit higher PH3 levels at centromeres, suggesting that dCAP-D3 is not involved in facilitating the directionality of condensation. Interestingly, we also observed that GFP-dCAP-D3 aggregates in prophase wing discs were consistently located next to PH3-dense (centromeric) chromosomal regions (Figure

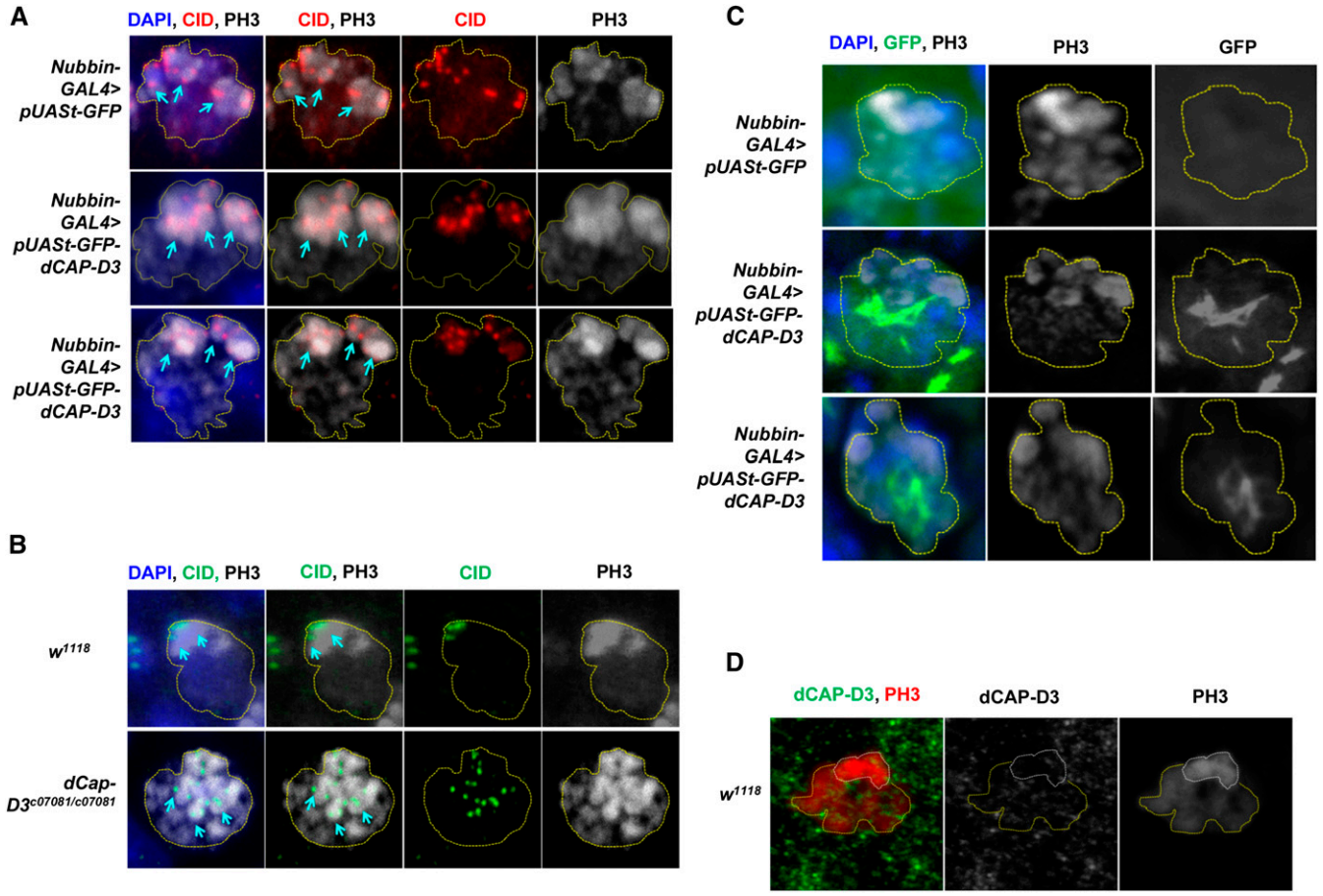

Figure 4 dCAP-D3 does not influence the directionality of condensation and localizes to less condensed mitotic DNA. (A) PH3 (gray) and CID (red) immunostaining in wing disc cells expressing GFP (*Nubbin-GAL4 > pUASt-GFP*) or GFP-dCAP-D3 (*Nubbin-GAL4 > pUASt-GFP-dCAP-D3*). DAPI staining of nuclei is shown in blue. Yellow dotted lines outline nuclear perimeter. (B) PH3 (gray) and CID (green) immunostaining in wild-type (w^{1118}) and *dCap-D3* mutant ($dCap\text{-}D3^{c07081/c07081}$) wing discs. DAPI staining of nuclei is shown in blue. Yellow dotted lines outline nuclear perimeter. (C) PH3 (gray) immunostaining in wing discs expressing control GFP (green, *Nubbin-GAL4 > pUASt-GFP*) or GFP-dCAP-D3 protein (green, *Nubbin-GAL4 > pUASt-GFP-dCAP-D3*). DAPI staining of nuclei is shown in blue. Yellow dotted lines outline nuclear perimeter. (D) Immunostaining for PH3 (red) and dCAP-D3 (green) in wild-type (w1118) wing discs. Yellow dotted line outlines less condensed DNA; white dotted line outlines more condensed DNA. Blue ← denote PH3-positive and CID-positive DNA.

4C), separating the more condensed from the less condensed DNA. This localization pattern was similar to that of endogenous dCAP-D3 in wild-type cells, which also appeared to aggregate, although in much smaller aggregations, and localize more strongly to less condensed DNA (Figure 4D)

As with the *dCap-D3* mutants, we also attempted to assess the effects of overexpression of dCAP-D3 on eclosion rates, as well as total body weight using the ubiquitous β-tubulin-GAL4 driver. However, the use of this driver to overexpress dCAP-D3 resulted in lethality at the pupal stage. Together, these data show that overexpression of dCAP-D3 can phenocopy dCAP-D3 deficiency in the regulation of mitotic timing, specifically in prophase, which could potentially contribute to developmental delays.

Overexpression of dCAP-D3 does not grossly affect genome organization in interphase

Interphase genome organization is also modulated by Condensin II. In fact, *Drosophila* dCAP-H2 overexpression has been linked to polytene chromosome disassembly, chromatin reorganization, and both centromeric and nuclear envelope defects (Hartl *et al.* 2008; Bauer *et al.* 2012; Buster *et al.* 2013). Furthermore, in *Drosophila* S2 cells, overexpression of dCAP-H2 has been shown to cause the compaction of individual chromosomes into globules during interphase (Buster *et al.* 2013). To test whether overexpression of dCAP-D3 would result in a similar phenotype, we transfected GFP-dCAP-D3 into S2 cells and stained cells with DAPI. While we did observe formation of GFP-dCAP-D3 nucleoplasmic aggregates, we did not see any gross changes to chromatin structure, as evidence by DAPI staining (Figure S9A). Overexpression of dCAP-H2 has been shown to result in nuclear envelope defects (Bozler *et al.* 2014). To test if dCAP-D3 overexpression would also result in similar defects, we immunostained salivary glands overexpressing dCAP-D3 with an antibody against lamin to visualize the nuclear envelope. These experiments, however, did not reveal any gross

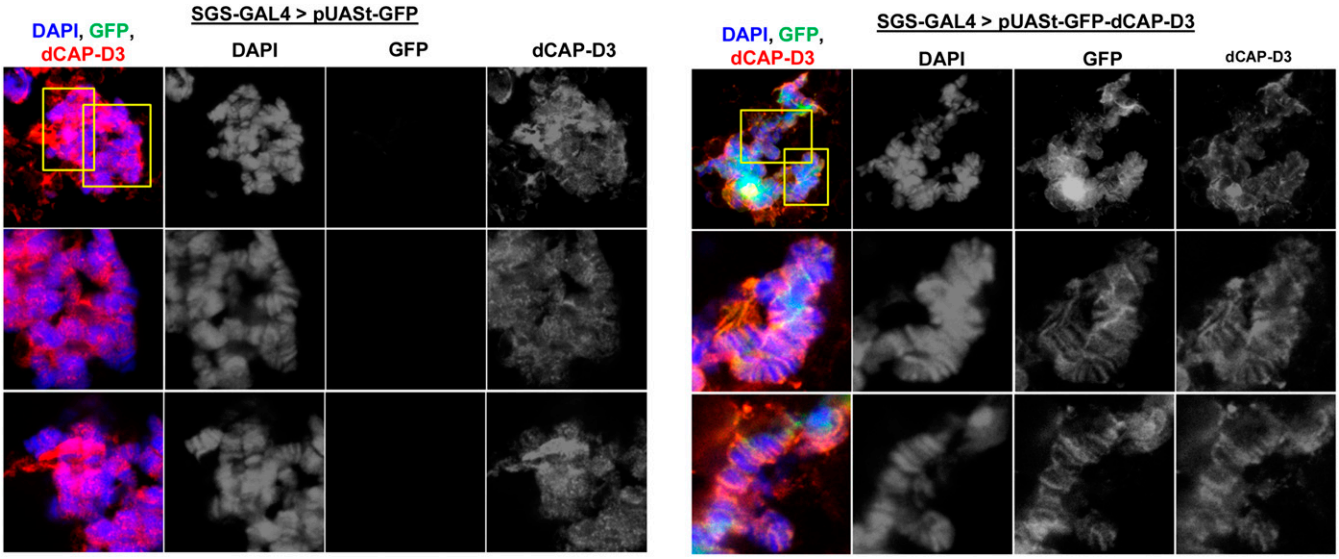

Figure 5 GFP-dCAP-D3 localizes to chromatin. Immunostaining for dCAP-D3 (red) of polytene squashes in salivary glands expressing control GFP (green, *SGS-GAL4 > pUASt-GFP*) or GFP-dCAP-D3 protein (green, *SGS-GAL4 > pUASt-GFP-dCAP-D3*). DAPI staining of DNA is shown in blue. First row shows full chromosome spread. Yellow box corresponds to close up in row 2. White box corresponds to close up in row 3.

changes to the nuclear envelope between GFP- and GFP-dCAP-D3-expressing cells (Figure S9B). Additionally, measurements revealed that dCAP-D3 overexpression did not have a significant effect on nuclear size (Figure S9C).

Since overexpression of dCAP-D3 did not result in gross changes to DNA morphology in S2 cells or *in vivo*, we wondered whether GFP-dCAP-D3 was localizing to DNA. To test this, polytene squashes were prepared from GFP and GFP-dCAP-D3 salivary glands and immunostained for dCAP-D3. Results revealed that GFP-dCAP-D3 does, in fact, localize to polytene chromatin in a pattern that does not overlap with DAPI dense regions, similar to what we have published previously for endogenous dCAP-D3 (Longworth *et al.* 2008) (Figure 5). Furthermore, IP of GFP-dCAP-D3 in salivary glands coupled with mass spectrometry successfully precipitated GFP-dCAP-D3 and identified a number of putative binding partners previously shown to associate with DNA, including Dodeca-satellite-binding protein 1 and histone H2B (Table 1). Surprisingly, we failed to coprecipitate GFP-dCAP-D3 and the other Condensin II subunits, however, this result is similar to experiments in which IP of dCAP-H2 in embryos and ovaries did not coprecipitate dCAP-D3, but did pull down dSMC4 and dSMC2 (Herzog *et al.* 2013). Taken together, these data suggest that dCAP-D3 aggregates formed upon overexpression in nondividing tissues did not seem to associate with the other Condensin II subunits and did not impart significant global changes to DNA organization in interphase.

dCAP-D3 overexpression results in deregulation of gene expression

Since our results showed that GFP-dCAP-D3 could localize to chromatin (Figure 5), we next tested the effects of overexpressing dCAP-D3 on gene expression in both the wing disc and salivary gland. While we have previously published that dCAP-D3 depletion results in transcriptional changes at the level of the whole organism (Longworth *et al.* 2012), gene targets of dCAP-D3 in wing disc and salivary glands have not been identified. Therefore, we performed RNA-seq in *dCap-D3*$^{c07081/c07081}$ third instar larval wing discs and salivary glands to identify targets specific to each tissue. From these experiments, in which dCAP-D3 levels were depleted, we identified 1781 and 1224 deregulated target genes in the salivary gland and wing disc, respectively, based on a logFC >1 (fold change >2) and FDR <0.05. (Figure 6A and Table S1). Wing disc and salivary gland samples could be separated by principal component analysis while dCAP-D3 expression status further partitioned samples within tissues (Figure S10). A total of 465 genes were found to be deregulated in both tissue types, with 119 concordantly upregulated and 274 concordantly downregulated. The remaining 72 shared target genes were deregulated in opposite directions in the two tissues (Figure 6B and Table S2).

GO analysis was performed to determine the types of gene programs and pathways affected by dCAP-D3 depletion (Figure 6C). The deregulation of genes involved in proteolysis, serine type endopeptidase activity, defense response to Gram-positive bacteria, oxidation reduction, iron and heme binding, oxidoreductase and monoxygenase activity, and chitin metabolism was observed in both tissues. Similar to what was previously published for the whole larvae, we observed that many of the deregulated immune response genes were actually upregulated when dCAP-D3 levels were depleted in the larval tissues, contrary to the downregulation we had previously reported in the adult fly (Longworth *et al.* 2012). This might be expected, as dCAP-D3 deficiency has been shown to result in chromosome instability in developing larval tissues and others have linked chromosome instability

Table 1 Putative binding partners of GFP-dCAP-D3

Gene name	Gene symbol	Accession number	Low salt		High salt	
			Con	IP	Con	IP
Chromosome-associated protein D3, isoform A	CAP-D3	24581942	16	391	0	34
Larval serum protein 1 gamma	Lsp1γ	17647601	10	112	21	126
Zipper, isoform B	zip	24762818	9	96	6	109
Heat shock protein cognate 3, isoform B	Hsc70-3	24641404	18	72	22	53
Heat shock protein cognate 4, isoform E	Hsc70-4	28571719	20	56	17	36
β-Coatomer protein	βCOP	17647193	0	54	0	5
Rudimentary, isoform A	r	24642586	0	43	0	0
Gamma-coatomer protein, isoform A	ϒCOP	17864148	0	39	0	3
Larval serum protein 1 β	Lsp1β	17136306	0	33	14	66
Oligosaccharide transferase Δ subunit	OstΔ	19922486	0	31	0	4
β′-Coatomer protein	β′COP	24584107	0	30	0	11
Ribosomal protein S27A	RpS27A	17136574	0	30	5	9
CG12715	CG12715	24641658	0	28	0	13
Calcium ATPase at 60A, isoform A	Ca-P60A	17136664	0	28	0	0
Glutamine–fructose-6-phosphate aminotransferase 2	Gfat2	21357745	0	26	0	2
Hemomucin	Hmu	17137194	0	21	0	15
Actin 87E, isoform A	Act87E	17137090	19	21	13	13
sec63	sec63	24660036	0	19	0	0
Regulatory particle non-ATPase 1	Rpn1	21356859	0	15	0	8
AP-1gamma, isoform A	AP-1γ	45549353	0	14	0	0
Eukaryotic translation initiation factor 4G, isoform A	eIF4G	161076325	0	14	0	0
UDP-N-acetyl-α-D-galactosamine:polypeptide N-acetylgalactosaminyltransferase 2, isoform A	GalNAc-T2	24643052	0	11	0	6
Veil	veil	19922444	0	10	1	11
CG30069	CG30069	116008309	3	10	0	0
Glycoprotein 93	Gp93	21357739	0	9	5	55
CG6453, isoform A	GCS2β	19921464	0	8	1	4
Karyopherin β 3, isoform A	Karyβ3	17737759	0	7	1	17
Polypeptide GalNAc transferase 6, isoform A	pgant6	24656262	0	7	0	3
Calnexin 99A, isoform A	Cnx99A	24651030	0	7	0	2
GalNAc-T1, isoform A	GalNAc-T1	19922324	0	7	0	2
Terribly reduced optic lobes, isoform L	trol	386763700	0	7	0	0
CG9318, isoform A	CG9318	19921598	0	6	0	0
Glutactin, isoform A	Glt	17137794	0	6	0	0
V-ATPase 69 subunit 2, isoform A	Vha68-2	24583984	0	5	3	53
Salivary gland secretion 3	Sgs3	17737563	1	5	1	24
CG30463, isoform A	CG30463	24654219	0	5	0	0
α-Coatomer protein, isoform B	αCOP	24655452	0	4	0	12
Aspartyl-tRNA synthetase, isoform C	Aats-asp	442623508	6	4	1	11
β-Adaptin	AP-1-2β	17647183	0	4	0	0
β-Tubulin at 56D, isoform B	βTub56D	24655737	0	4	0	0
α-Tubulin at 84B	αTub84B	17136564	0	3	0	0
GTP-binding protein	Gtp-bp	24641198	0	3	0	0
White	w	17136592	0	3	0	0
Δ-Coatomer protein, isoform A	δCOP	21355081	0	2	0	8
Regulatory particle non-ATPase 2, isoform A	Rpn2	24650984	0	2	0	8
SLY-1 homologous, isoform C	Slh	45552183	0	2	0	0
Coro, isoform A	coro	24586098	2	1	9	12
Mitochondrial trifunctional protein α-subunit, isoform A	Mtpα	19921000	0	1	0	7
PolyA-binding protein, isoform C	pAbp	24654797	0	1	0	4
Glutamyl-prolyl-tRNA synthetase, isoform A	Aats-glupro	24649466	0	1	0	3
Heat shock protein 83, isoform A	Hsp83	17647529	0	0	17	94
Elongation factor 2b, isoform A	EF2	24585709	0	0	9	86
Tudor-SN, isoform A	Tudor-SN	20130403	0	0	0	47
CG3523, isoform A	FASN1	19920632	0	0	0	36
TER94, isoform C	TER94	161076486	0	0	2	36
CG8036, isoform D	CG8036	24645119	0	0	3	34
CG1516, isoform G	PCB	24652216	0	0	0	17
Ghost, isoform B	Sec24CD	442625387	0	0	0	17
Protein disulfide isomerase, isoform A	Pdi	17647799	0	0	1	17

(continued)

Table 1, *continued*

Gene name	Gene symbol	Accession number	Low salt		High salt	
			Con	IP	Con	IP
Threonyl-tRNA synthetase, isoform A	Aats-thr	24583839	0	0	3	17
ATP citrate lyase, isoform D	ATPCL	281363473	0	0	0	15
Dodeca-satellite-binding protein 1, isoform C	Dp1	24655003	0	0	0	13
Glycyl-tRNA synthetase, isoform A	Aats-gly	21357965	0	0	0	12
Histone H2B	His2b	24585671	0	0	0	12
Isoleucyl-tRNA synthetase, isoform A	Aats-ile	24668543	0	0	0	12
Heat shock protein 60, isoform A	Hsp60	24641191	0	0	1	9
Alanyl-tRNA synthetase, isoform B	Aats-ala	45552267	0	0	0	7
Larval serum protein 1 alpha	Lsp1α	24641542	0	0	0	7
Vacuolar H[+] ATPase subunit 100-2, isoform B	Vha100-2	21357019	0	0	0	7
CG33123	CG33123	28574733	0	0	0	6
Kinesin heavy chain	Khc	17136240	0	0	0	6
CG7461	CG7461	281363737	0	0	0	5
Hsc70Cb, isoform A	Hsc70Cb	21357475	0	0	0	5
α-Actinin, isoform C	Actn	17137758	0	0	0	4
CG17259, isoform A	CG17259	24581334	0	0	0	4
Ecto-5′-nucleotidase 2, isoform A	NT5E-2	19922446	0	0	0	4
eIF3-S10	eIF3-S10	24643988	0	0	0	4
sec23, isoform B	sec23	24644351	0	0	0	3
CG8258	CG8258	19921848	0	0	0	2
eIF3-S9, isoform B	eIF3-S9	19922458	0	0	0	2
CG9010	CG9010	19922412	0	0	6	0

tRNA, transfer RNA.

with activation of innate immune signaling in *Drosophila* wing discs (Longworth *et al.* 2008; Liu *et al.* 2015). While not tested, changes in chromatin landscape at different stages of development (*i.e.*, adult *vs.* larval stage) could also account for the change in the direction of deregulation. While most GO terms unique to the wing disc included immune response genes, structural proteins, and extracellular matrix genes, uniquely enriched GO terms in the salivary glands included flavonoid processes and response to insecticide/DTT.

Randomly chosen upregulated targets were validated by qRT-PCR in tissue from both *dCap-D3*$^{c07081/c07081}$ and *dCap-D3*$^{c07081/\Delta 25}$ larvae (Figure 6, D and E). The *Δ25* deletion is a genomic deletion on the second chromosome that encompasses *dCap-D3* and was expressed to confirm the observed changes in transcript levels were not due to bystander allele effect. Results from qRT-PCR experiments confirmed that the transcript levels of dCAP-D3 target genes identified by RNA-seq were changed in the expected direction.

Finally, to test whether dCAP-D3 overexpression affected target gene expression, qRT-PCR was performed on cDNA synthesized from RNA isolated from salivary glands and wing discs expressing GFP or GFP-dCAP-D3. In salivary glands, we found that overexpression of dCAP-D3 resulted in the downregulation of three target genes (*CG32071*, *CG32073*, and *CG13560*) whose expression was upregulated in dCAP-D3-deficient tissue (Figure 6F). We observed a similar phenomenon in the wing disc, with dCAP-D3 overexpression resulting in the downregulation of three target genes (*CecC*, *CG13560*, and *HP1D3csd*) whose expression was upregulated in dCAP-D3-deficient tissue (Figure 6G). These data demonstrate that overexpression of dCAP-D3 results in the deregulation of gene expression in both dividing and nondividing tissues and can occur in a manner that is opposite to what is observed when dCAP-D3 levels are depleted.

Discussion

Prior to this work, the effects of elevated dCAP-D3 expression on the major functions of Condensin II, including mitosis, DNA organization, and transcriptional regulation, were unknown. However, our findings that elevated levels of CAP-D3 are found in many somatic cancers clearly demonstrates that elevated levels of CAP-D3, regardless of the reason for these higher levels, could have very important biological consequences. Our data now show that in *Drosophila*, overexpression of dCAP-D3 in developing larval tissues results in the formation of nucleoplasmic aggregates that act in a dominant-negative manner to slow mitotic prophase, similar to what is observed in dCAP-D3-deficient tissue. Interestingly, and in contrast to events observed in dCAP-D3-deficient tissues, overexpression of dCAP-D3 accelerates the metaphase to anaphase transition, and it is also during this period that the nucleoplasmic aggregates disappear. Notably, alterations to mitotic timing are only observed in cells harboring GFP-dCAP-D3 aggregates, which suggests it is the physical aggregation of the protein that is required for this phenotype. Future studies examining human tumor samples for the presence of CAP-D3 aggregates will reveal more about how and why these aggregates are formed. Our findings also demonstrate that while dCAP-D3 overexpression does not seem to affect global chromosome organization during interphase, it does result in changes to transcript levels of dCAP-D3 target

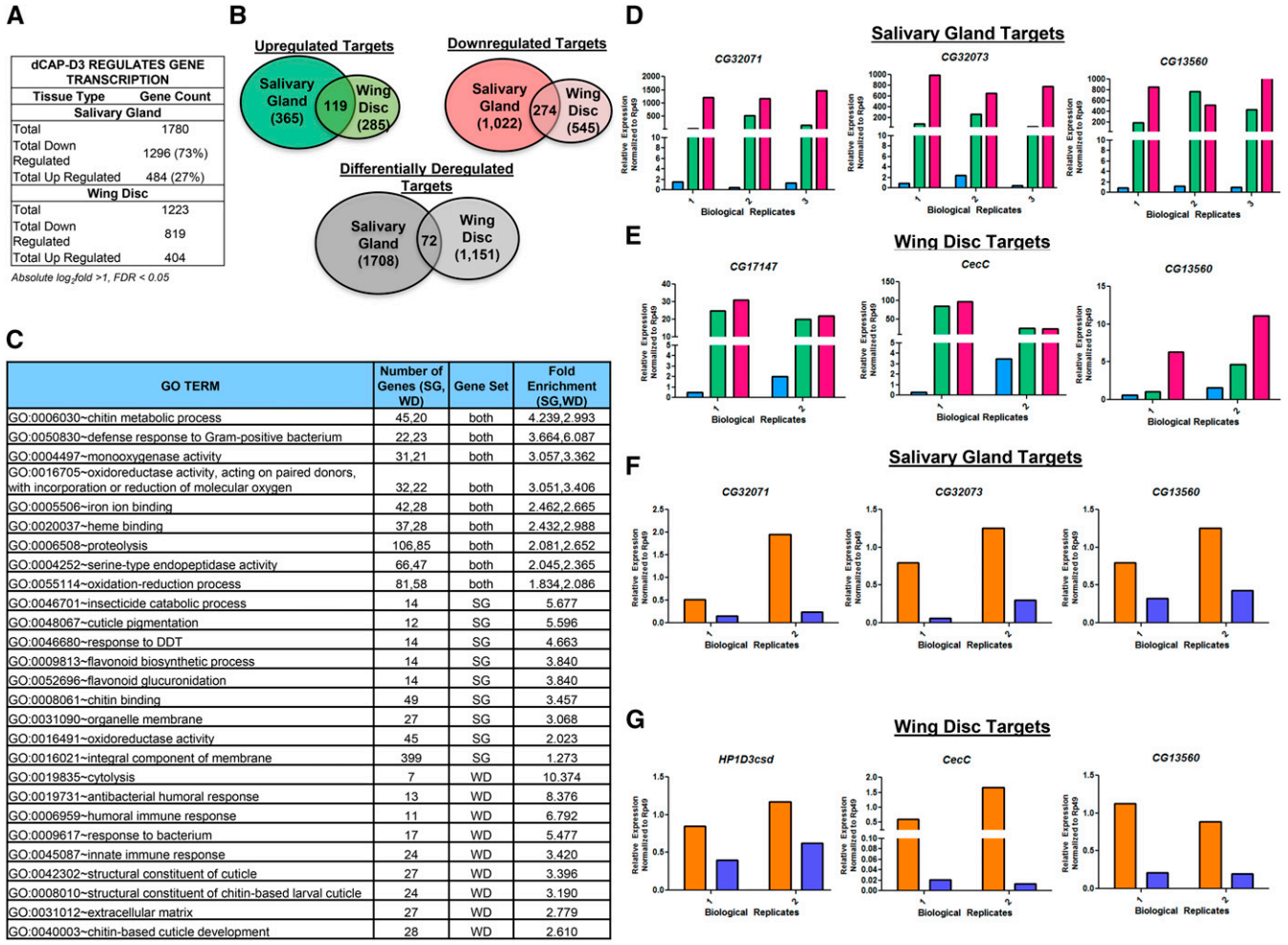

GO TERM	Number of Genes (SG, WD)	Gene Set	Fold Enrichment (SG,WD)
GO:0006030~chitin metabolic process	45,20	both	4.239,2.993
GO:0050830~defense response to Gram-positive bacterium	22,23	both	3.664,6.087
GO:0004497~monooxygenase activity	31,21	both	3.057,3.362
GO:0016705~oxidoreductase activity, acting on paired donors, with incorporation or reduction of molecular oxygen	32,22	both	3.051,3.406
GO:0005506~iron ion binding	42,28	both	2.462,2.665
GO:0020037~heme binding	37,28	both	2.432,2.988
GO:0006508~proteolysis	106,85	both	2.081,2.652
GO:0004252~serine-type endopeptidase activity	66,47	both	2.045,2.365
GO:0055114~oxidation-reduction process	81,58	both	1.834,2.086
GO:0046701~insecticide catabolic process	14	SG	5.677
GO:0048067~cuticle pigmentation	12	SG	5.596
GO:0046680~response to DDT	14	SG	4.663
GO:0009813~flavonoid biosynthetic process	14	SG	3.840
GO:0052696~flavonoid glucuronidation	14	SG	3.840
GO:0008061~chitin binding	49	SG	3.457
GO:0031090~organelle membrane	27	SG	3.068
GO:0016491~oxidoreductase activity	45	SG	2.023
GO:0016021~integral component of membrane	399	SG	1.273
GO:0019835~cytolysis	7	WD	10.374
GO:0019731~antibacterial humoral response	13	WD	8.376
GO:0006959~humoral immune response	11	WD	6.792
GO:0009617~response to bacterium	17	WD	5.477
GO:0045087~innate immune response	24	WD	3.420
GO:0042302~structural constituent of cuticle	27	WD	3.396
GO:0008010~structural constituent of chitin-based larval cuticle	24	WD	3.190
GO:0031012~extracellular matrix	27	WD	2.779
GO:0040003~chitin-based cuticle development	28	WD	2.610

Figure 6 Overexpression of dCAP-D3 regulates gene expression in larval salivary glands and wing discs. (A) Table summarizing the number of deregulated genes identified from RNA-seq experiment performed in dCAP-D3-deficient (*dCap-D3*$^{c07081/c07081}$) salivary glands and wing discs. Significant targets were identified based on a logFC >1 (fold change >2), FDR <0.05. For salivary glands, three biological replicates were used for both wild-type (*w*^{1118}) and *dCap-D3* mutant (*dCap-D3*$^{c07081/c07081}$) samples. For wing discs, three biological replicates were used for wild-type (*w*^{1118}) and two for *dCap-D3* mutant (*dCap-D3*$^{c07081/c07081}$) samples. (B) Venn diagrams showing the number of unique and shared upregulated (green), downregulated (red), and discordantly (gray) altered dCAP-D3 target genes. (C) Summary of DAVID GO analysis of genes presented in (A) using FDR <0.05. (D and E) qRT-PCR validation of three upregulated dCAP-D3 target genes identified from RNA-seq in the (D) salivary glands and (E) wing discs (blue is *w*^{1118}, green is *dCap-D3*$^{c07081/c07081}$, pink is *dCap-D3*$^{c07081/\Delta 25}$). (F and G) qRT-PCR in GFP- (orange) and GFP-dCAP-D3- (purple) expressing (F) salivary glands and (G) wing discs to detect transcript levels of dCAP-D3 target genes. SG = salivary glands, WD = wing discs.

genes in an opposite manner to changes observed in dCAP-D3-deficient tissues. Furthermore, should CAP-D3 overexpression have a conserved effect in human somatic tumors, these phenomena could lead to inefficient partitioning of daughter chromosomes and/or deregulation of important homeostatic transcriptional programs which could further promote tumorigenesis.

A major question that arises from this work is whether or not the dCAP-D3 aggregates possess significant functions that directly affect cellular homeostasis. Our studies are not the first to describe aggregation of Condensin II proteins upon overexpression. CAP-H2 overexpression in human cells was previously shown to result in the formation of aggregates that colocalize with markers of senescence-associated heterochromatin foci, and knockdown of CAP-H2 was subsequently found to inhibit oncogene-induced senescence (Yokoyama *et al.* 2015). The fact that, in our studies, dCAP-D3 aggregates are present in dividing cells as they enter into mitosis, however, argues against the fact that they play a role in senescence. Additionally, immunofluorescence experiments showed that dCAP-D3 aggregates did not appear to colocalize with heterochromatin markers in salivary glands (data not shown).

Our data correlating the disappearance of the dCAP-D3 aggregates at the metaphase to anaphase transition with a change in the observed effects of dCAP-D3 overexpression on mitotic timing suggests that the aggregates may interfere with the condensation functions of the Condensin II complex, but this dominant-negative effect is lost once the aggregates disappear. This effect is also not observed when aggregates

were not present from the onset of prophase. One possibility is that the dCAP-D3 aggregates may be amplifying our ability to visualize a structure that is actually present in cells expressing normal levels of CAP-D3. Figure 4 shows that dCAP-D3 aggregates present in mitotic wing disc cells are localized proximal to, but not overlapping with, DNA that is heavily stained with PH3 (*i.e.*, more condensed DNA). In fact, the aggregates seem to separate the more condensed DNA from the less condensed DNA. Interestingly, immunostaining performed with primary antibody to dCAP-D3 in mitotic wing disc cells shows the appearance of structures that look like much smaller aggregates of dCAP-D3 protein, suggesting that these aggregates can form from endogenously expressed dCAP-D3 protein, although at a drastically reduced level (Figure 4). Recently, using double-stranded DNA tethered to a surface, yeast Condensins were shown to use the energy provided from ATP hydrolysis to extrude DNA loops in real time (Ganji *et al.* 2018). These studies provided *in vitro* evidence for a model in which the kleisin and HEAT-repeat subunits of the Condensin complex could anchor a DNA strand at one region and then extrude the rest of the strand through the Condensin ring. Another recent article combined Hi-C data from synchronized chicken DT-40 cells with polymer simulations to examine the formation of mitotic chromosomes (Gibcus *et al.* 2018). These studies showed that immediately following entry into mitosis, chromosomes lose their interphase organization and are folded into arrays of loops positioned around a central axis (Gibcus *et al.* 2018). Excitingly, they also demonstrated that Condensin II is required for both the formation of the loop arrays and for reorganization of the arrays in prometaphase into shapes that resemble spiral staircases. If these phenomena are conserved and applicable to the configuration of chromosomes in *Drosophila* wing discs in prophase/prometaphase, then GFP-dCAP-D3 overexpression may allow us to visualize Condensin II complexes organizing the mitotic DNA into condensed, helical loop arrays on the centromere-proximal side of the Condensin II aggregate network, and the less condensed, potentially less looped DNA on the telomere-proximal side. In this scenario, the abnormally high levels of dCAP-D3 could result in a tighter association with DNA, making it harder for Condensin II to move along the DNA as it is being progressively looped and condensed, thus increasing the duration of prophase. Further studies involving overexpression of CAP-D3 proteins unable to bind to Condensin II subunits, combined with Hi-C analyses in these cells, will help to confirm or refute these hypotheses.

The cell-specific mechanisms that regulate formation of dCAP-D3 aggregates and the mechanisms that facilitate their disappearance remain unknown. dCAP-H2 is degraded by the Slimb ubiquitin ligase in *Drosophila*, but Slimb does not affect levels of dCAP-D3 (Buster *et al.* 2013). To date, a similar mechanism involved in dCAP-D3 degradation has not been identified. Alternative to active degradation of dCAP-D3 protein occurring at the onset of metaphase, it is also possible that the GFP-dCAP-D3 aggregates are breaking down due to diffusion of the protein away from the nucleus, since *Drosophila* cells have been shown to undergo a partial nuclear envelope breakdown at the end of prophase (Paddy *et al.* 1996).

Recently, *Drosophila* Condensin II was shown to promote the separation of sister chromatids during interphase in Cohesin-depleted cells, in line with Condensin II's known role as an antipairer (Senaratne *et al.* 2016). Our data also show that when dCAP-D3 is overexpressed and aggregates are present, the protein behaves differently after the onset of metaphase after the aggregates have disappeared, resulting in phenotypes that are opposite to those seen in cells deficient for dCAP-D3 expression. Since we observe an acceleration in the transition from metaphase to anaphase when dCAP-D3 is overexpressed (Figure 3), it is possible that dCAP-D3 may act to speed up sister chromatid separation, thus significantly decreasing the timing of this mitotic window.

Whether Condensin II's condensation and transcriptional regulatory functions are linked currently remains an unanswered question in the field. Evidence exists suggesting that defects in condensation can directly affect gene expression (Rawlings *et al.* 2011); however, whether Condensin II subunits can influence transcription through an alternative mechanism has never been directly tested. In our studies, we observe that overexpression of dCAP-D3 results in changes to target gene transcript levels that are opposite to those observed in dCAP-D3-deficient tissues (Figure 6). It is possible that all observed changes in transcriptional regulation could be a result of disruption to local nuclear architecture. For example, depletion of dCAP-D3 could cause local decondensation, while overexpression could cause local hyper-condensation, thus resulting in transcriptional changes in opposing directions. However, IP-mass spectrometry experiments performed by both our laboratory (Table 1) and others fail to show that overexpressed dCAP-D3 protein associates with other Condensin II members. Therefore, during interphase, it is possible that dCAP-D3 could be regulating gene expression through a secondary mechanism, independently of Condensin II. Further support for this idea is the fact that overexpression of dCAP-D3 in interphase cells does not result in similar phenotypes caused by dCAP-H2 overexpression. Additional studies aimed at identifying key residues needed to cause the phenotypes associated with dCAP-D3 overexpression and for association with Condensin II would provide insight as to how intertwined its condensation/Condensin II-specific and gene regulatory functions truly are.

Finally, aberrant expression and activity of Condensin II has been linked to a number of diseases, including cancer. Both loss of Condensin II subunits and disruption of their loading onto chromatin in mice has been reported to drive lymphomagenesis (Atchison 2014; Woodward *et al.* 2016; Ishak *et al.* 2017). Here, we report data derived from the COSMIC database, which show that expression levels of Condensin II subunits are more commonly elevated than decreased in many somatic tumors (Figure 1), and TCGA data showing elevated Condensin II levels correlate with lower survival rates in patients with low-grade glioma (Figure S1, A–C). Additionally,

increased levels of CAP-G2 correlate with poor prognosis in cases of nonsmall cell lung cancer (Zhan *et al.* 2017). Condensin II subunit depletion in several organisms has been shown to result in lagging chromosomes and increases in DNA damage (Hartl *et al.* 2008; Longworth *et al.* 2008; Lee *et al.* 2011; Green *et al.* 2012; Schuster *et al.* 2013; Bakhrebah *et al.* 2015). Our *in vivo* studies demonstrate that dCAP-D3 overexpression causes an acceleration of the metaphase to anaphase transition. In other studies, this has been shown to result in the bypassing of the spindle checkpoint, which can lead to increases in chromosome missegregation and aneuploidy (Meraldi *et al.* 2004). Future analyses of lagging chromosome generation and karyotypes in human cells overexpressing CAP-D3 would determine whether the increased metaphase to anaphase transition leads to chromosomal instability. It is also possible that higher CAP-D3 levels may promote tumorigenesis through the aberrant regulation of genes necessary for the development and the maintenance of homeostasis. Our data provide insight into how overexpression of the genome-organizing protein dCAP-D3 affects cellular homeostasis in both mitosis and in interphase and, if conserved, these findings could shed light on the possible mechanisms by which elevated CAP-D3 levels could influence tumor development and/or tumor progression.

Acknowledgments

We thank Kavitha Sarvepalli for assistance with tissue collections, members of the Longworth laboratory, Lerner Research Institute Imaging Core, George Aranjuez, Christian Lehner, and John Poulton (Peifer laboratory) for advice and assistance with protocols and design of experiments. We thank Gary Karpen for the generous donation of CID antibody. Stocks were obtained from the Bloomington *Drosophila* Stock Center (National Institutes of Health P40 OD-018537). We thank Helen Salz and all Longworth laboratory members for helpful advice and comments on the manuscript. We thank Courtney Hershberger, Richard Padgett, Xuan Guo, and Hua Lou for assistance in analyzing and understanding aspects of RNA-sequencing data. This work was supported by the National Institutes of Health (GM-102400 to M.S.L., 1S10RR026820 to the Lerner Research Institute Imaging Core, and 1S10RR031537-01 to the Lerner Research Institute Proteomics Core) and a Velo-Sano Cancer Research Award to M.S.L. The funders had no role in study, design, data collection, analysis, decision to publish, or preparation of the manuscript. The authors declare no competing or financial interests.

Literature Cited

Abe, S., K. Nagasaka, Y. Hirayama, H. Kozuka-Hata, M. Oyama *et al.*, 2011 The initial phase of chromosome condensation requires Cdk1-mediated phosphorylation of the CAP-D3 subunit of condensin II. Genes Dev. 25: 863–874. https://doi.org/10.1101/gad.2016411

Anders, S., P. T. Pyl, and W. Huber, 2015 HTSeq–a Python framework to work with high-throughput sequencing data. Bioinformatics 31: 166–169. https://doi.org/10.1093/bioinformatics/btu638

Apte, M. S., and V. H. Meller, 2012 Homologue pairing in flies and mammals: gene regulation when two are involved. Genet. Res. Int. 2012: 430587. https://doi.org/10.1155/2012/430587

Atchison, M. L., 2014 Function of YY1 in long-distance DNA interactions. Front. Immunol. 5: 45. https://doi.org/10.3389/fimmu.2014.00045

Bakhrebah, M., T. Zhang, J. R. Mann, P. Kalitsis, and D. F. Hudson, 2015 Disruption of a conserved CAP-D3 threonine alters condensin loading on mitotic chromosomes leading to chromosome hypercondensation. J. Biol. Chem. 290: 6156–6167. https://doi.org/10.1074/jbc.M114.627109

Bauer, C. R., T. A. Hartl, and G. Bosco, 2012 Condensin II promotes the formation of chromosome territories by inducing axial compaction of polyploid interphase chromosomes. PLoS Genet. 8: e1002873. https://doi.org/10.1371/journal.pgen.1002873

Blower, M. D., and G. H. Karpen, 2001 The role of *Drosophila* CID in kinetochore formation, cell-cycle progression and heterochromatin interactions. Nat. Cell Biol. 3: 730–739. https://doi.org/10.1038/35087045

Bolzer, A., G. Kreth, I. Solovei, D. Koehler, K. Saracoglu *et al.*, 2005 Three-dimensional maps of all chromosomes in human male fibroblast nuclei and prometaphase rosettes. PLoS Biol. 3: e157. https://doi.org/10.1371/journal.pbio.0030157

Bozler, J., H. Q. Nguyen, G. C. Rogers, and G. Bosco, 2014 Condensins exert force on chromatin-nuclear envelope tethers to mediate nucleoplasmic reticulum formation in Drosophila melanogaster. G3 (Bethesda) 5: 341–352. https://doi.org/10.1534/g3.114.015685

Buster, D. W., S. G. Daniel, H. Q. Nguyen, S. L. Windler, L. C. Skwarek *et al.*, 2013 SCFSlimb ubiquitin ligase suppresses condensin II-mediated nuclear reorganization by degrading Cap-H2. J. Cell Biol. 201: 49–63. https://doi.org/10.1083/jcb.201207183

Cremer, T., and M. Cremer, 2010 Chromosome territories. Cold Spring Harb. Perspect. Biol. 2: a003889. https://doi.org/10.1101/cshperspect.a003889

Croft, J. A., J. M. Bridger, S. Boyle, P. Perry, P. Teague *et al.*, 1999 Differences in the localization and morphology of chromosomes in the human nucleus. J. Cell Biol. 145: 1119–1131. https://doi.org/10.1083/jcb.145.6.1119

Dekker, J., and L. Mirny, 2016 The 3D genome as moderator of chromosomal communication. Cell 164: 1110–1121. https://doi.org/10.1016/j.cell.2016.02.007

dos Santos, G., A. J. Schroeder, J. L. Goodman, V. B. Strelets, M. A. Crosby *et al.*, 2015 FlyBase: introduction of the Drosophila melanogaster Release 6 reference genome assembly and large-scale migration of genome annotations. Nucleic Acids Res. 43: D690–D697. https://doi.org/10.1093/nar/gku1099

Dowen, J. M., and R. A. Young, 2014 SMC complexes link gene expression and genome architecture. Curr. Opin. Genet. Dev. 25: 131–137. https://doi.org/10.1016/j.gde.2013.11.009

Dowen, J. M., S. Bilodeau, D. A. Orlando, M. R. Hübner, B. J. Abraham *et al.*, 2013 Multiple structural maintenance of chromosome complexes at transcriptional regulatory elements. Stem Cell Rep. 1: 371–378. https://doi.org/10.1016/j.stemcr.2013.09.002

Forbes, S. A., D. Beare, H. Boutselakis, S. Bamford, N. Bindal *et al.*, 2017 COSMIC: somatic cancer genetics at high-resolution. Nucleic Acids Res. 45: D777–D783. https://doi.org/10.1093/nar/gkw1121

Ganji, M., I. A. Shaltiel, S. Bisht, E. Kim, A. Kalichava *et al.*, 2018 Real-time imaging of DNA loop extrusion by condensin. Science 360: 102–105. https://doi.org/10.1126/science.aar7831

Gibcus, J. H., K. Samejima, A. Goloborodko, I. Samejima, N. Naumova *et al.*, 2018 A pathway for mitotic chromosome formation. Science 359: eaao6135. https://doi.org/10.1126/science.aao6135

Gorkin, D. U., D. Leung, and B. Ren, 2014 The 3D genome in transcriptional regulation and pluripotency. Cell Stem Cell 14: 762–775. https://doi.org/10.1016/j.stem.2014.05.017

Green, L. C., P. Kalitsis, T. M. Chang, M. Cipetic, J. H. Kim *et al.*, 2012 Contrasting roles of condensin I and condensin II in mitotic chromosome formation. J. Cell Sci. 125: 1591–1604. https://doi.org/10.1242/jcs.097790

Ham, M. F., T. Takakuwa, N. Rahadiani, K. Tresnasari, H. Nakajima *et al.*, 2007 Condensin mutations and abnormal chromosomal structures in pyothorax-associated lymphoma. Cancer Sci. 98: 1041–1047. https://doi.org/10.1111/j.1349-7006.2007.00500.x

Handke, B., J. Szabad, P. V. Lidsky, E. Hafen, and C. F. Lehner, 2014 Towards long term cultivation of Drosophila wing imaginal discs in vitro. *PLoS One* 9: e107333. https://doi.org/10.1371/journal.pone.0107333

Hartl, T. A., S. J. Sweeney, P. J. Knepler, and G. Bosco, 2008a Condensin II resolves chromosomal associations to enable anaphase I segregation in Drosophila male meiosis. PLoS Genet. 4: e1000228. https://doi.org/10.1371/journal.pgen.1000228

Hartl, T. A., H. F. Smith, and G. Bosco, 2008b Chromosome alignment and transvection are antagonized by condensin II. Science 322: 1384–1387. https://doi.org/10.1126/science.1164216

Hendzel, M. J., Y. Wei, M. A. Mancini, A. Van Hooser, T. Ranalli *et al.*, 1997 Mitosis-specific phosphorylation of histone H3 initiates primarily within pericentromeric heterochromatin during G2 and spreads in an ordered fashion coincident with mitotic chromosome condensation. Chromosoma 106: 348–360. https://doi.org/10.1007/s004120050256

Herzog, S., S. Nagarkar Jaiswal, E. Urban, A. Riemer, S. Fischer *et al.*, 2013 Functional dissection of the Drosophila melanogaster condensin subunit cap-G reveals its exclusive association with condensin I. PLoS Genet. 9: e1003463. https://doi.org/10.1371/journal.pgen.1003463

Hirota, T., D. Gerlich, B. Koch, J. Ellenberg, and J.-M. Peters, 2004 Distinct functions of condensin I and II in mitotic chromosome assembly. J. Cell Sci. 117: 6435–6445. https://doi.org/10.1242/jcs.01604

Holwerda, S., and W. de Laat, 2012 Chromatin loops, gene positioning, and gene expression. Front. Genet. 3: 217. https://doi.org/10.3389/fgene.2012.00217

Huang, D. W., B. T. Sherman, and R. A. Lempicki, 2009 Systematic and integrative analysis of large gene lists using DAVID bioinformatics resources. Nat. Protoc. 4: 44–57. https://doi.org/10.1038/nprot.2008.211

Ishak, C. A., C. H. Coschi, M. V. Roes, and F. A. Dick, 2017 Disruption of CDK-resistant chromatin association by pRB causes DNA damage, mitotic errors, and reduces condensin II recruitment. Cell Cycle 16: 1430–1439. https://doi.org/10.1080/15384101.2017.1338984

Joyce, E. F., B. R. Williams, T. Xie, and C.-T. Wu, 2012 Identification of genes that promote or antagonize somatic homolog pairing using a high-throughput FISH-based screen. PLoS Genet. 8: e1002667. https://doi.org/10.1371/journal.pgen.1002667

Kim, D., G. Pertea, C. Trapnell, H. Pimentel, R. Kelley *et al.*, 2013 TopHat2: accurate alignment of transcriptomes in the presence of insertions, deletions and gene fusions. Genome Biol. 14: R36. https://doi.org/10.1186/gb-2013-14-4-r36

Klebanow, L. R., E. C. Peshel, A. T. Schuster, K. De, K. Sarvepalli *et al.*, 2016 Drosophila condensin II subunit chromosome-associated protein D3 regulates cell fate determination through non-cell-autonomous signaling. Development 143: 2791–2802. https://doi.org/10.1242/dev.133686

Lee, J., S. Ogushi, M. Saitou, and T. Hirano, 2011 Condensins I and II are essential for construction of bivalent chromosomes in mouse oocytes. Mol. Biol. Cell 22: 3465–3477. https://doi.org/10.1091/mbc.e11-05-0423

Leiserson, M. D., F. Vandin, H. T. Wu, J. R. Dobson, J. V. Eldridge *et al.*, 2015 Pan-cancer network analysis identifies combinations of rare somatic mutations across pathways and protein complexes. Nat. Genet. 47: 106–114. https://doi.org/10.1038/ng.3168

Li, H., and R. Durbin, 2009 Fast and accurate short read alignment with Burrows-Wheeler transform. Bioinformatics 25: 1754–1760. https://doi.org/10.1093/bioinformatics/btp324

Li, L., X. Lyu, C. Hou, N. Takenaka, H. Q. Nguyen *et al.*, 2015 Widespread rearrangement of 3D chromatin organization underlies polycomb-mediated stress-induced silencing. Mol. Cell 58: 216–231. https://doi.org/10.1016/j.molcel.2015.02.023

Link, J., D. Paouneskou, M. Velkova, A. Daryabeigi, T. Laos *et al.*, 2018 Transient and partial nuclear lamina disruption promotes chromosome movement in early meiotic prophase. Dev. Cell 45: 212–225.e7. https://doi.org/10.1016/j.devcel.2018.03.018

Liu, D., Z. Shaukat, R. B. Saint, and S. L. Gregory, 2015 Chromosomal instability triggers cell death via local signalling through the innate immune receptor Toll. Oncotarget 6: 38552–38565. https://doi.org/10.18632/oncotarget.6035

Longworth, M. S., A. Herr, J. Y. Ji, and N. J. Dyson, 2008 RBF1 promotes chromatin condensation through a conserved interaction with the condensin II protein dCAP-D3. Genes Dev. 22: 1011–1024. https://doi.org/10.1101/gad.1631508

Longworth, M. S., J. A. Walker, E. Anderssen, N. S. Moon, A. Gladden *et al.*, 2012 A shared role for RBF1 and dCAP-D3 in the regulation of transcription with consequences for innate immunity. PLoS Genet. 8: e1002618. https://doi.org/10.1371/journal.pgen.1002618

Lupiáñez, D. G., K. Kraft, V. Heinrich, P. Krawitz, F. Brancati *et al.*, 2015 Disruptions of topological chromatin domains cause pathogenic rewiring of gene-enhancer interactions. Cell 161: 1012–1025. https://doi.org/10.1016/j.cell.2015.04.004

Lupiáñez, D. G., M. Spielmann, and S. Mundlos, 2016 Breaking TADs: how alterations of chromatin domains result in disease. Trends Genet. 32: 225–237. https://doi.org/10.1016/j.tig.2016.01.003

McCarthy, D. J., Y. Chen, and G. K. Smyth, 2012 Differential expression analysis of multifactor RNA-Seq experiments with respect to biological variation. Nucleic Acids Res. 40: 4288–4297. https://doi.org/10.1093/nar/gks042

Meraldi, P., V. M. Draviam, and P. K. Sorger, 2004 Timing and checkpoints in the regulation of mitotic progression. Dev. Cell 7: 45–60. https://doi.org/10.1016/j.devcel.2004.06.006

Nasmyth, K., and C. H. Haering, 2005 The structure and function of SMC and kleisin complexes. Annu. Rev. Biochem. 74: 595–648. https://doi.org/10.1146/annurev.biochem.74.082803.133219

Nora, E. P., J. Dekker, and E. Heard, 2013 Segmental folding of chromosomes: a basis for structural and regulatory chromosomal neighborhoods? BioEssays 35: 818–828. https://doi.org/10.1002/bies.201300040

Ono, T., A. Losada, M. Hirano, M. P. Myers, A. F. Neuwald *et al.*, 2003 Differential contributions of condensin I and condensin II to mitotic chromosome architecture in vertebrate cells. Cell 115: 109–121. https://doi.org/10.1016/S0092-8674(03)00724-4

Ono, T., Y. Fang, D. L. Spector, and T. Hirano, 2004 Spatial and temporal regulation of Condensins I and II in mitotic chromosome assembly in human cells. Mol. Biol. Cell 15: 3296–3308. https://doi.org/10.1091/mbc.e04-03-0242

Paddy, M. R., H. Saumweber, D. A. Agard, and J. W. Sedat, 1996 Time-resolved, in vivo studies of mitotic spindle formation and nuclear lamina breakdown in Drosophila early embryos. J. Cell Sci. 109: 591–607.

Pan, X., M. Papasani, Y. Hao, M. Calamito, F. Wei *et al.*, 2013 YY1 controls Igκ repertoire and B-cell development, and localizes with condensin on the Igκ locus. EMBO J. 32: 1168–1182. https://doi.org/10.1038/emboj.2013.66

Poulton, J. S., J. C. Cuningham, and M. Peifer, 2014 Acentrosomal Drosophila epithelial cells exhibit abnormal cell division, leading to cell death and compensatory proliferation. Dev. Cell 30: 731–745. https://doi.org/10.1016/j.devcel.2014.08.007

Rawlings, J. S., M. Gatzka, P. G. Thomas, and J. N. Ihle, 2011 Chromatin condensation via the condensin II complex is required for peripheral T-cell quiescence. EMBO J. 30: 263–276. https://doi.org/10.1038/emboj.2010.314

Risso, D., J. Ngai, T. P. Speed, and S. Dudoit, 2014 Normalization of RNA-seq data using factor analysis of control genes or samples. Nat. Biotechnol. 32: 896–902. https://doi.org/10.1038/nbt.2931

Schuster, A. T., K. Sarvepalli, E. A. Murphy, and M. S. Longworth, 2013 Condensin II subunit dCAP-D3 restricts retrotransposon mobilization in Drosophila somatic cells. PLoS Genet. 9: e1003879. https://doi.org/10.1371/journal.pgen.1003879

Schuster, A. T., C. R. Homer, J. R. Kemp, K. P. Nickerson, E. Deutschman *et al.*, 2015 Chromosome-associated protein D3 promotes bacterial clearance in human intestinal epithelial cells by repressing expression of amino acid transporters. Gastroenterology 148: 1405–1416.e3. https://doi.org/10.1053/j.gastro.2015.02.013

Senaratne, T. N., E. F. Joyce, S. C. Nguyen, and C. T. Wu, 2016 Investigating the interplay between sister chromatid cohesion and homolog pairing in Drosophila nuclei. PLoS Genet. 12: e1006169. https://doi.org/10.1371/journal.pgen.1006169

Smallwood, A., and B. Ren, 2013 Genome organization and long-range regulation of gene expression by enhancers. Curr. Opin. Cell Biol. 25: 387–394. https://doi.org/10.1016/j.ceb.2013.02.005

Steffensen, S., P. A. Coelho, N. Cobbe, S. Vass, M. Costa *et al.*, 2001 A role for Drosophila SMC4 in the resolution of sister chromatids in mitosis. Curr. Biol. 11: 295–307. https://doi.org/10.1016/S0960-9822(01)00096-3

Thibault, S. T., M. A. Singer, W. Y. Miyazaki, B. Milash, N. A. Dompe *et al.*, 2004 A complementary transposon tool kit for Drosophila melanogaster using P and piggyBac. Nat. Genet. 36: 283–287. https://doi.org/10.1038/ng1314

Van Bortle, K., and V. G. Corces, 2012 Nuclear organization and genome function. Annu. Rev. Cell Dev. Biol. 28: 163–187. https://doi.org/10.1146/annurev-cellbio-101011-155824

Woodward, J., G. C. Taylor, D. C. Soares, S. Boyle, D. Sie *et al.*, 2016 Condensin II mutation causes T-cell lymphoma through tissue-specific genome instability. Genes Dev. 30: 2173–2186. https://doi.org/10.1101/gad.284562.116

Xu, Y., C. G. Leung, D. C. Lee, B. K. Kennedy, and J. D. Crispino, 2006 MTB, the murine homolog of condensin II subunit CAP-G2, represses transcription and promotes erythroid cell differentiation. Leukemia 20: 1261–1269. https://doi.org/10.1038/sj.leu.2404252

Yokoyama, Y., H. Zhu, R. Zhang, and K. Noma, 2015 A novel role for the condensin II complex in cellular senescence. Cell Cycle 14: 2160–2170. https://doi.org/10.1080/15384101.2015.1049778

Yuen, K. C., B. D. Slaughter, and J. L. Gerton, 2017 Condensin II is anchored by TFIIIC and H3K4me3 in the mammalian genome and supports the expression of active dense gene clusters. Sci. Adv. 3: e1700191. https://doi.org/10.1126/sciadv.1700191

Zhan, P., G. M. Xi, B. Zhang, Y. Wu, H. B. Liu *et al.*, 2017 NCAPG2 promotes tumour proliferation by regulating G2/M phase and associates with poor prognosis in lung adenocarcinoma. J. Cell. Mol. Med. 21: 665–676. https://doi.org/10.1111/jcmm.13010

Communicating editor: B. Calvi